ISSN 2723-6471

Design of a Green City with Lower Carbon Based on Vegetation in Banjarbaru using Sentinel-2

Hanifah Dwi Nirwana[1,*], Akhmad Rizalli Saidy[2], Gusti Muhammad Hatta[3], Agung Nugroho[4]

[1]*Doctoral Program of Agricultural Sciences, Lambung Mangkurat University, Banjarbaru, South Kalimatan 70714, Indonesia*

[2]*Department of Soil, Faculty of Agriculture, Lambung Mangkurat University, Banjarbaru, South Kalimatan 70714, Indonesia*

[3]*Departement of Forestry Science, Faculty of Forestry, Lambung Mangkurat University, Banjarbaru, South Kalimatan 70714, Indonesia*

[4]*Department of Agro-Industrial Technology, Faculty of Agriculture, Lambung Mangkurat University, Banjarbaru, South Kalimatan 70714, Indonesia*

(Received: February 8, 2024; Revised: March 15, 2024; Accepted: April 20, 2024; Available online: May 31, 2024)

Abstract

In addressing the pervasive issue of Urban Heat Islands (UHI) and the related carbon sequestration challenges in urban settings, this study utilizes Sentinel-2 imagery to propose a vegetative blueprint for the design green city with lower carbon in Banjarbaru. This research intricately links the role of increased vegetation cover in mitigating UHI effects and enhancing carbon absorption in urban environments. By employing a combination of Geographic Information Systems (GIS), field data, and real-time data via Wireless Sensor Networks (WSN), the study highlights the significant cooling and environmental benefits of strategically increasing green spaces in urban areas. Moreover, the study identifies specific zones within Banjarbaru that are optimal for the strategic placement of vegetation to maximize thermal comfort and carbon storage. This focus on localized green infrastructure development not only provides a pathway to more sustainable urban living conditions but also serves as a model for other cities facing similar ecological and climatic challenges. The integrated approach adopted here emphasizes continuous monitoring and dynamic adjustments in urban planning, ensuring long-term sustainability and resilience against the ongoing threats posed by climate change and urban expansion.

Keywords: Heat Islands, Sentinel-2, GIS; WSN, Thermal Comfort, Carbon Storage

1. Introduction

Global warming represents a formidable challenge to environmental sustainability, exacerbated by urbanization and industrialization which intensify local and global climate dynamics. The melting of polar ice caps, a salient indicator of global warming, has precipitated a concerning rise in global sea level from an annual increase of 2.2 ± 0.3 mm in 1993 to 3.3 ± 0.3 mm by 2014, indicating an alarming acceleration in oceanic volume expansion [1], [2]. This phenomenon not only symbolizes the dire state of polar regions but also underscores a broader environmental destabilization, driven predominantly by greenhouse gas (GHG) emissions. These emissions, primarily from urban sectors, encapsulate solar radiation, thereby elevating terrestrial temperatures and altering global precipitation patterns—a process substantially contributing to the UHI effect [3], [4]

Urban centers, due to dense population and infrastructural developments, are major contributors to GHG emissions. Cities like Sydney, Calgary, and Stuttgart see per capita emissions exceeding 15 tons of CO2-equivalent, starkly contrasting with lower emissions in cities within Nepal, India, and Bangladesh [5]. The UHI phenomenon, first identified by Luke Howard in 1810, exemplifies the thermal alterations urban areas undergo, primarily due to land cover changes and pollution [6]. These urban heat islands not only elevate local temperatures but also degrade urban living conditions and ecological resilience, making the development of sustainable urban infrastructure imperative [7].

***Corresponding author: Hanifah Dwi Nirwana (2240511320002@mhs.ulm.ac.id)**
DOI: https://doi.org/10.47738/jads.v5i2.218

 ISSN 2723-6471

Recognizing the urgent need to address GHG emissions, international bodies and local governments are advocating for Low Carbon Cities (LCC). Initiatives such as ICLEI's Green Climate Cities program and The World Business Council for Sustainable Development's Urban Infrastructure Initiative aim to facilitate sustainable urban planning and GHG management. Concurrently, national strategies, including Indonesia's Medium-Term National Development Plan 2020–2024, emphasize integrating climate protection policies into broader developmental agendas. This holistic approach seeks to blend environmental stewardship with urban development, striving to not only mitigate UHI effects but also enhance the global resilience against climate change [8].

Building on the outlined environmental and urban challenges, it is essential to contextualize the pressing issues that our research aims to address. This study is prompted by critical questions regarding the impact of UHI effects on urban livability, the role of vegetation in carbon sequestration and UHI mitigation, and the effective design patterns necessary for developing low-carbon green cities based on land cover concepts. These considerations lead directly to the study's objectives, which include analyzing UHI impacts on residential comfort, exploring land cover's role in enhancing carbon absorption and reducing UHI effects, and designing low-carbon green urban spaces.

The goals of this research are intricately linked to its expected benefits, particularly in providing insights into the role of vegetation in reducing UHI zones and enhancing urban living spaces. Additionally, this study aims to offer a clear concept and design for a low-carbon city based on land cover, which could serve as a crucial reference in urban planning for Banjarbaru and other cities aiming to reduce UHI effects and improve urban comfort. By addressing these aspects, the research seeks not only to contribute to the academic field, but also to offer practical solutions for urban sustainability and resilience against climate change.

In the context of Banjarbaru, a green city refers to an urban area designed to optimize green spaces, reduce carbon emissions, and enhance residents' quality of life through strategic vegetation planting and the use of green technologies. This includes the implementation of international standards such as ICLEI's Green Climate Cities program and the World Business Council for Sustainable Development's Urban Infrastructure Initiative.

Moreover, our research boundaries are well-defined, focusing exclusively on Banjarbaru's administrative region and considering variables such as surface and air temperatures, humidity, and carbon absorption. This focused approach allows us to develop a comprehensive spatial model that will include data from satellite imagery, field data, and WSN [9], providing robust insights into thermal comfort and urban greenery's effectiveness in mitigating UHI effects. This methodological framework sets the stage for a novel contribution to the field, emphasizing the need for integrated social and biological considerations in urban forest functions and low-carbon city development, addressing gaps identified in previous studies.

2. Method

This research is predicated on a clearly defined problem that has been preliminarily explored through an extensive literature review, subsequently informing the formulation of specific research objectives and the underlying methodological approach. To facilitate a comprehensive understanding of this study, a conceptual framework has been delineated as presented in figure 1.

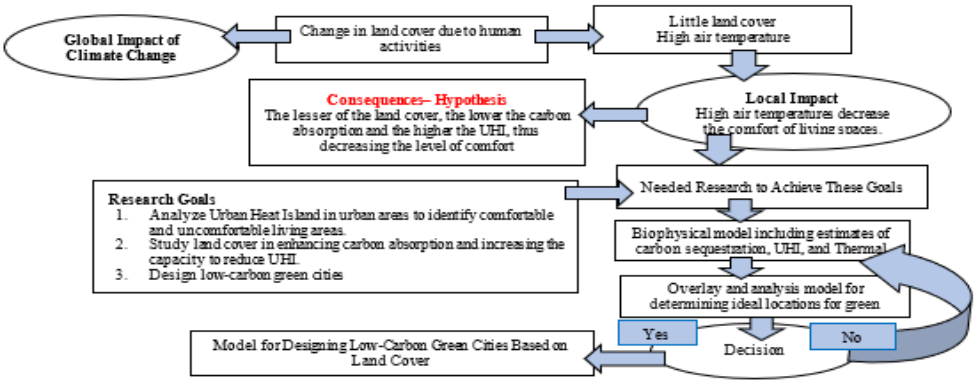

Figure 1. Research Framework

This research focuses on geospatial analysis using Quantum Geographic Information System (QGIS) software and field surveys conducted in the city of Banjarbaru, South Kalimantan Province. QGIS was selected for its capability in detailed spatial analysis and compatibility with Sentinel-2 data. Thermohygrometers are used for accurate measurement of temperature and humidity in the field, which is crucial for UHI analysis [10]. One of the main challenges in field measurements is the variation in weather conditions that can affect the accuracy of temperature and humidity data. To address this issue, measurements are conducted at multiple time points to obtain more representative data.

2.1. Stages of Research Implementation

The UHI analysis employs tools such as Q-GIS (Raster calculator), Microsoft Excel, GRASS GIS, and SAGA GIS, along with applications like Avenza/GPS-RTK, thermal cameras, thermohygrometers, and WSNs. Data collection combines literature study and field surveys, with specific formulas used for data analysis, such as the LST calculated as: $Ts=Tb/(1+\lambda(Tb/a)\ln(\varepsilon))$, and UHI determined by $UHI = Tmean – (\mu + 0.5\ \alpha)$ [11]. Brightness temperature and Temperature Humidity Index (THI) are also calculated using respective formulas. For the analysis of land cover and carbon absorption, tools like Q-GIS (Reclass), roll meters, sample rings, and drones are used. NDVI [3], [10] is calculated using NDVI = (NIR - Red) / (NIR + Red), and carbon volume is estimated through the formula C-tree = $(0.5\pi(D/2)^2$ * form factor (0.7) * carbon fraction (0.5))/1,000. The project also entails designing a low-carbon city based on land cover, utilizing tools like Microsoft Excel and baseline maps, with data gathered from literature and field surveys and analyzed using overlay models for carbon absorption, LST, UHI, and thermal comfort [12].

The measurement of greenhouse gas emissions, carbon sequestration, and carbon stocks is conducted at sample points placed proportionally within each NDVI class based on their respective areas, with a sampling intensity of 0.1%. The number of plots in this study is determined following the sample points consist of 20m x 20m (400 m²) sampling plots, totaling four pixels per plot (as shown in Figure 1), using Sentinel-2 imagery. The total number of sample plots is adjusted proportionally to the predefined sample area size. Plots are strategically placed using purposive sampling distributed across each NDVI class, ensuring that the pixel values surrounding each sample plot are consistent with adjacent pixel values to minimize sampling errors. Sample plots are then mapped and entered into the Global Positioning System to serve as a reference for field surveys shown in figure 2.

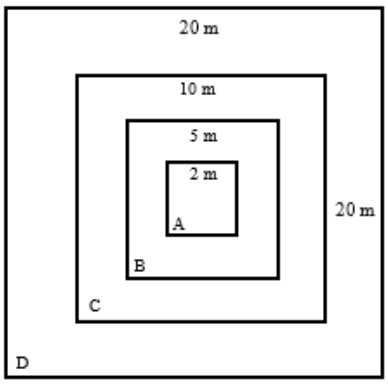

Figure 2. Research Plot Form

This sample plot delineates the sampling areas for various measurement levels: tree level in a 20x20m area, pole level in a 10x10m area, stake level in a 5x5m area, seedling level in a 2x2m area, and litter level in a 1x1m area. These plot sizes are applied across both peat and mineral soils. The position for sampling data such as land surface temperature, humidity, light intensity, thermal comfort, and other supporting parameters is aligned with the NDVI sample point locations. However, if the positions do not coincide, separate sample plots are established by selecting points four times within a 5-meter radius around the NDVI sample points. Sampling on peat and mineral land areas. By combining these two sampling methods, the accuracy of the research data is enhanced. Field observations are also conducted at the sample plot locations. Observations involve recording physical factors that influence the UHI phenomenon. Field criteria include the type of land surface cover, land use and allocation, building roof types and the number of floors, as well as the nature and type of vegetation and the condition of Green Open Spaces [13], [14], [15].

2.2. Data Analysis

Primary data, both in the form of satellite images and field data, are analyzed to obtain research results. The data analysis process for this research includes:

2.2.1. Downloading Sentinel-2 Imagery

Sentinel-2 imagery can be downloaded for free through earthexplorer.usgs.gov. The images are selected for the Banjarbaru area with cloud cover below 20% and are also chosen from the most recent recording year.

2.2.2. Radiometric and Atmospheric Calibration

Radiometric correction is necessary to improve the visual quality of images and to correct pixel values that do not match the actual spectral reflectance values of objects [16]. Atmospheric correction aims to reduce object reflectance after normalizing lighting conditions and removing atmospheric traces. In the Sentinel-2A imagery, geometric and radiometric corrections are systematically performed by Sentinel. However, when processing in the QGIS application, the manual equation that can be elaborated is [17]:

$$\text{Wavelenght Citra Sentinel} = \frac{\text{Digital Number (DN)}}{\text{Solar irradiance}} \quad (1)$$

2.2.3. Transformation NDVI (Normalized Difference Vegetation Index)

The NDVI transformation is used to determine the vegetation index in the study area by displaying the degree of greenness of the vegetation as an indicator of biomass density. NDVI also serves to differentiate between vegetation and non-vegetation objects based on the absorption of received wavelengths [18]. In this study, NDVI is an indicator used to measure the presence and density of vegetation in urban areas. NDVI information is utilized to analyze the relationship between vegetation and surface temperature, as well as carbon absorption. The data in this study uses Sentinel-2 satellite imagery and CO2 data using a WSN with a CO2 Infra-Red DF Robot sensor device. Therefore, the NIR and Red bands are used for extraction. NDVI is formulated as follows:

$$\text{NDVI} = \frac{\text{NIR Band} - \text{Red Band}}{\text{NIR Band} + \text{Red Band}} \quad (2)$$

Note: NIR Band = Band NIR from Sentinel-2, Red Band = Band Red from Sentinel-2

The NDVI value has a classification range from -1 to 1. NDVI values that represent vegetation fall within the range of 0.1 to 1. NDVI values less than zero indicate the presence of covers such as clouds, non-vegetative objects, and water. The following are the NDVI classification range values [19] presented in table 1 below.

Table 1. NDVI Class

NDVI value	NDVI class	Land cover
1	-0,9 – 0,00	Cloud, Water
2	0,00 – 0,10	Open Area, Mine
3	0,10 – 0,20	Meadow
4	0,20 – 0,30	Shrub
5	0,30 – 0,40	Young plantation
6	0,40 – 0,50	Old Plantation, Young Secondary Forest
7	0,50 – 0,60	Medium Secondary Forest
8	0,60 – 0,70	Young Secondary Forest

2.2.4. Land Surface Temperature (LST)

LST is the Earth's surface temperature measured or estimated using remote sensing data from satellites. In this dataset, LST refers to the actual temperature experienced at the surface of the ground, vegetation, and buildings. In the context

of this research, LST is a parameter used to analyze and model the distribution patterns of temperature in urban areas [16]. LST is measured or estimated using satellite imagery data that reflects the thermal radiation intensity from the Earth's surface. In this study, LST is used as an input variable in modeling and the data obtained also includes ground temperature and humidity from a DS18B20 sensor, air temperature and humidity from a DHT11 sensor, and thermal camera data. Land surface temperature can be calculated by reducing brightness temperature and considering surface emissivity values. The emissivity values for each land cover type are as follows: water bodies at 0.979, built-up lands at 0.965, open lands at 0.964, and vegetated lands at 0.986 [4]. The formula for surface temperature is provided by USGS:

$$Ts = \frac{Tb}{1 + \lambda \left(\frac{Tb}{a}\right) \ln (\varepsilon)} \quad (3)$$

note:

Ts = Surface temperature (K)

Tb = Brightness temperature (K)

λ = The mean value of the channel wavelength (11.5 µm)

a = hc/k (148380 K)

h = Constanta planck (6.26 x 10-34 Js)

c = Speed of light (2.998 x 108 ms-1)

k = Constanta Stefan Boltzman (1.38 x 10-23 JK-1)

Ɛ = Emisisvity Object

2.2.5. Urban Heat Island

UHI data can be obtained from the extraction of Sentinel-2 satellite imagery by deriving Land Surface Temperature (LST) data. UHI maps can be produced by modifying the existing equations and incorporating the following formula as [16]:

$$UHI = T_{mean} - (\mu + 0{,}5\ \alpha) \quad (4)$$

note:

UHI = Urban Heat Island

Tmean = Land Surface Temperature (ºCelcius)

µ = Average value LST (ºCelcius)

α = Veviation Value Standart LST (ºCelcius)

Meanwhile, UHI is divided into 3 classes which are presented in table 2.

Table 2. UHI Class

UHI Class	Range of UHI
1	0 – 2 °C
2	2 – 4 °C
3	>4 °C

2.2.6. Thermal Humidity Index (THI)

The most commonly used measurement for thermal comfort is the THI, which has been applied in various studies and is a relevant index for assessing thermal comfort in tropical regions. The equation for THI is as follows:

$$THI = 0{,}8\ Ta + (RH\ x\ Ta\ /\ 500) \quad (5)$$

Note:

THI = Thermal Humidity Index

Ta = Air Temperature (°C)

RH = Relative Humidity (%)

2.2.7. Spatial Regression Modeling

In this research, spatial regression is employed as the analytical method to model the relationship between dependent variables, such as land surface temperature and humidity, and independent variables, such as land cover, building density, or proximity to heat sources, within the spatial analysis context of the UHI model for low-carbon city design. This method is crucial for considering the spatial structure of data, helping identify factors influencing UHI in low-carbon city designs based on land cover. Below is the formula for Spatial Regression [20]:

1) Notation:
   Y(u): Value of the response variable at the prediction location

   X(u): Value of the predictor variable at the prediction location

   $Y(x_i)$: Value of the response variable at observation location i

   $X(x_i)$: Value of the predictor variable at observation location i

   ε(u): Residual at the prediction location

   β: Regression coefficient

2) Spatial Value Estimation

$$(Y(u)): Y(u)=X(u)\beta+\epsilon(u) Y(u)=X(u)\beta+\epsilon(u) \quad (6)$$

3) Regression Coefficient

$$(\beta): \beta=(X'WX)-1X'WY \beta=(X'WX)-1X'WY \quad (7)$$

In this formulation, Y(u) represents the predicted value of the response variable at the prediction location. X(u) represents the values of the predictor variables used to predict the response variable at that location. $Y(x_i)$ and $X(x_i)$ represent the values of the response and predictor variables at observation location i, respectively. ε(u) is the residual, the difference between the actual observed value and the value predicted by the regression model.

The steps in the spatial regression analysis for this study include:

1) Data Collection Using WSN: Installing temperature sensors at various locations to measure ground surface temperature and humidity.
2) Model Building: Constructing a spatial regression model that considers predictor variables like land cover, building density, or distance to heat sources. This regression model will estimate the relationships between these predictors and land surface temperature in the design of low-carbon green cities.
3) Model Evaluation and Interpretation: Evaluating and interpreting the regression model to understand the relative impacts of the predictor variables on land surface temperature.

2.2.8. Validation Test

The estimated carbon potential from the developed model is then compared with the carbon potential information from each testing plot. The comparison or accuracy testing method used is the Root Mean Square Error, which is calculated as follows:

$$RMSE = \frac{\sqrt{(Xi - Yi)^2}}{n} \quad (8)$$

 ISSN 2723-6471

Note:

RMSE = Root Mean Square Error

Yi represents the estimated necromass data from the i-th pixel of the correlation model

Xi represents the actual necromass data on the i-th plot from the testing area

n is the number of testing sample plots

3. Result and Discussion

Greenhouse gases, such as CO2, absorb and emit infrared radiation, leading to an increase in atmospheric temperatures. The following diagram illustrates how GHGs are trapped in the atmosphere, increasing the Earth's surface temperature. Data from literature, field surveys, and WSN are combined through an overlay process in Q-GIS to produce comprehensive maps. This analysis ensures that all data sources are considered, enhancing the accuracy and validity of the research results. NDVI was chosen for its proven ability to measure vegetation density and its relationship with carbon sequestration. Although there are other vegetation indices, NDVI offers the best balance between ease of use and accuracy in the context of this research.

Mitigating UHI through increased green spaces can improve residents' quality of life by providing recreational areas and reducing energy costs for cooling. Carbon sequestration by vegetation also has the potential to be developed as a carbon trading project, providing additional economic benefits to the local community. The proposed green city design in Banjarbaru can be applied to other cities with similar geographic and climatic conditions, such as Palangkaraya and Samarinda. This vegetation-based approach can be adapted to various urban scales. The findings of this study are compared with similar studies in tropical cities like Jakarta and Kuala Lumpur. The results indicate similar challenges and solutions in reducing UHI effects through increased green spaces.

Based on the research findings, it is recommended that the Banjarbaru city government invest more in green infrastructure, including tree planting along streets and the development of city parks, to reduce UHI effects and enhance carbon sequestration.

3.1. Urban Heat Island Analysis in Cities

To obtain information on the level of residential comfort (THI), an analysis LST is necessary from the Land Surface Temperature data, patterns of heat distribution, known as UHI effect, can be determined. This analysis could help identifying areas with elevated temperatures compared to their surroundings, which are typically more uncomfortable for living due to higher heat retention. Understanding these patterns is crucial for addressing urban planning and public health concerns related to thermal comfort in residential areas.

3.1.1. Land Surface Temperature (LST)

The analysis of land surface temperature was conducted using Sentinel-2 imagery and direct field measurements. The results are presented in Table 3 as result from sentinel-2.

Table 3. Result from analysis of land surface temperature was conducted using Sentinel-2

Number Plot	Digital Value Sentinel 2A (ºC)	Soil temperature from field measurements (ºC)
13	27,7	30,9
14	27,4	30,9
48	25,9	30,1
36	26,1	29,7
37	27,7	29,7
8	27,1	29,4
38	27,0	29,4

 ISSN 2723-6471

46	25,8	29,2
18	26,3	29,1
33	24,9	28,8
49	25,2	27,9
54	24,4	27,9
34	24,6	27,7
68	25,5	27,7
6	24,1	27,3
60	24,9	27,3
67	24,3	27,3
58	23,9	27,1
63	24,4	27,1
62	24,4	27,0
66	23,9	27,0
57	24,4	26,9
56	23,0	26,3

Based on table 3, a graph was constructed to model the relationship between field-measured land surface temperatures derived from Sentinel-2 imagery and those measured directly on the ground. The coefficient of determination (R^2) obtained was 0.835, indicating a very strong correlation. Figure 3 below show illustration between field-measured soil temperatures and Sentinel 2.

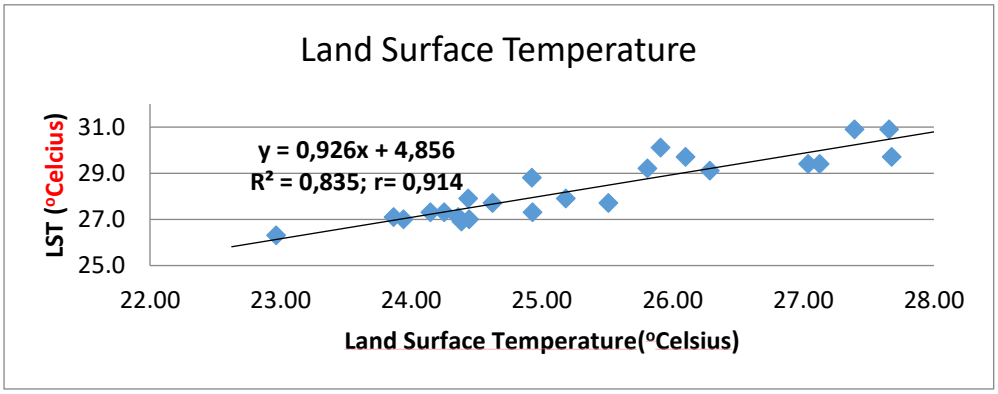

Figure 3. Graph of the relationship between field-measured soil temperatures and Sentinel 2

The graph illustrates the relationship between LST and field soil temperature, where LST is measured in degrees Celsius. There is a positive correlation between the two variables, as depicted by the linear regression line with the equation y=0.926x+4.856. The coefficient of determination, R^2, is 0.835, indicating that about 83.5% of the variation in LST can be explained by the field soil temperature variable. The correlation between these variables is quite strong with an r value of 0.914, close to 1, indicating a very significant statistical relationship between field temperatures and measured land surface temperatures. This Results show that an increase in field soil temperature tends to be followed by an increase in LST. This equation is then used to predict the surface temperature values in the research area. The results shown in figure 4.

 ISSN 2723-6471

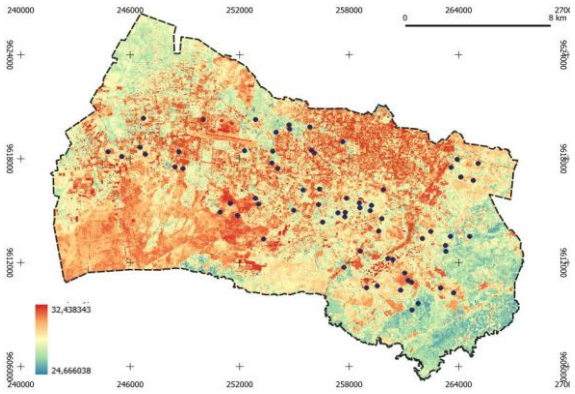

Figure 4. Land Surface Temperature

This map of land surface temperature shows the distribution of temperatures in Banjarbaru in September 2023, as analyzed from LST data using Sentinel-2 satellite imagery. The highest temperature reaches 32.44°C in urban areas, generally concentrated in the western part of the region. Urban areas with high building density or open land without vegetation cover often trigger the UHI phenomenon [13]. Conversely, the lowest recorded temperature is 24.67°C and is more dominant in areas with denser vegetation, such as parks, forests, or agricultural areas that help maintain lower temperatures. Surface temperature variability in urban areas is influenced by land cover and land use, where surfaces like concrete and asphalt absorb and retain more heat compared to natural environments [6], [17], [18]. Vegetated areas, which typically have cooler surface temperatures, contribute to cooler air temperatures. Research has shown that land cover changes, such as a decrease in urban vegetation and an increase in population, can enhance anthropogenic heat emissions contributing to the intensity of the urban heat island [8]. Moreover, the spatial pattern of land cover also affects surface temperatures, where the transformation of natural landscapes into urban settlements can cause significant temperature increases compared to surrounding.

Other studies have highlighted the importance of vegetation in reducing the urban heat island effect by showing that the presence of green spaces can help reduce surface temperatures and affect temperature patterns in urban areas. Furthermore, changes in land cover have also been shown to impact surface temperature distribution, where areas with natural forest cover or parks have lower temperatures compared to densely urbanized areas. Thus, research on the relationship between land cover, changes in surface temperature, and the effects of the urban heat island becomes crucial in the context of sustainable urban planning and adaptation to climate change [8], [19], [20].

3.1.2. Urban Heat Island (UHI)

Based on the LST values, the UHI index was calculated, and the results are presented in the following figure 5.

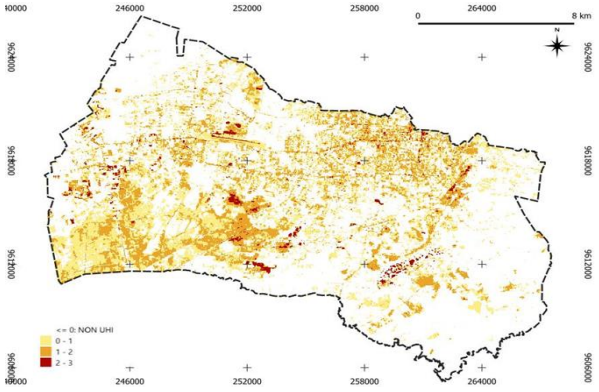

Figure 5. Urban Heat Island (UHI) Distribution Pattern

Figure 5 shows a thematic map that illustrates the distribution of the UHI effect in the urban area of Banjarbaru, using Sentinel-2 image data from September 2023. Non-UHI areas, which do not show increased temperatures, are characterized by lighter, almost white colors, indicating regions with a temperature increase of 0 degrees, typically areas with good vegetation cover or open spaces unaffected by urban heat. UHI Class 1 (0-1 degrees), represented by

 ISSN 2723-6471

pale yellow, includes urban areas with slight temperature increases due to urban development but still retaining some vegetation or open spaces. UHI Class 2 (1-2 degrees), shown in a darker yellow, marks areas with moderate heat intensity possibly caused by a mix of urban infrastructure and lack of vegetation cover. Finally, UHI Class 3 (2-3 degrees), marked in brown to reddish tones, indicates regions with significant temperature increases, usually associated with densely urbanized areas such as city centers or industrial zones with minimal vegetation. This map is useful for urban planners to identify heat zones and plan UHI mitigation strategies, such as enhancing green spaces or designing more efficient buildings.

UHI is a phenomenon where urban areas experience significantly higher temperatures than surrounding rural areas. Urbanization and climate change have exacerbated this issue, sparking an urgent need to reduce its impacts through UHI mitigation in urban planning. Various UHI mitigation strategies have been proposed, such as the development of green spaces and changes in building materials to reduce the negative impacts of UHI and address future challenges.

Other research shows that urban characteristics, local meteorological conditions, and the presence of green spaces influence UHI intensity. Moreover, the transition from rural landscapes to urban areas triggers UHI. In this context, it is vital to monitor the impacts of UHI to support sustainable urban planning [21].

UHI mitigation has become a critical topic across various fields such as urban ecology, urban planning, urban geography, and urban meteorology. UHI mitigation strategies, such as cool roofs and indoor temperature adjustments, can help reduce near-surface air temperatures and heat stress for residents. However, there is a planning dilemma regarding whether dense urban development is a viable UHI mitigation strategy.

3.1.3. Temperature Humidity Index (THI)

From the LST values supported by humidity data, the THI values are derived. Graphically, from these calculations, a map depicting the distribution of THI values is obtained as shown in figure 6 below.

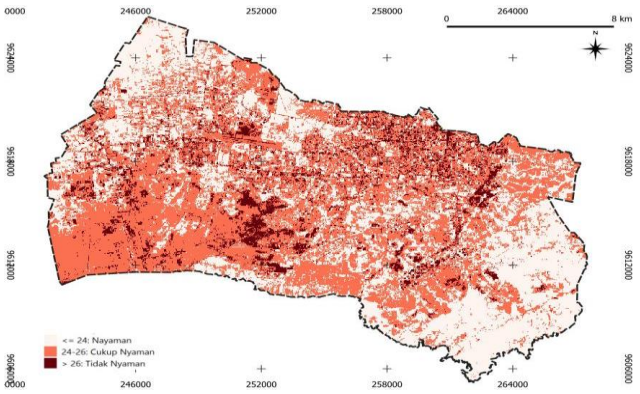

Figure 6. Distribution Pattern of Temperature Humidity Index (THI)

Figure 6 presents the analysis of the THI in the Banjarbaru area, based on Sentinel-2 imagery for September 2023. THI is an indicator used to assess thermal comfort based on temperature and humidity. This map illustrates the thermal comfort index, reflecting comfort conditions based on temperature in a region. Areas with a THI up to 24 degrees, characterized by the lightest color on the map, are considered "Comfortable" zones and are primarily located in the eastern and western parts of the region. These zones may have dense vegetation or geographical features that support lower temperatures. Areas with a THI between 24 and 26 degrees are marked with a medium color and are grouped in the "Moderately Comfortable" class. This indicates areas with moderate climatic conditions that may already be influenced by urban factors such as asphalt and concrete that absorb heat. Regions with a THI above 26 degrees, marked by the darkest color, are classified as "Uncomfortable." These areas typically include densely developed urban regions, open areas, water bodies, and scrubland that tend to have higher temperatures due to a lack of vegetation or the direct effects of solar heating. This map is useful for policymakers and urban planners to target greening and cooling interventions in uncomfortable areas and to optimize comfort in urban and open zones.

The Thermal Comfort Index compiled based on temperature and humidity has a significant impact on community life. THI is used to evaluate the thermal environment for both humans and animals, as temperature and humidity have

interactive effects on thermal comfort. Studies have shown that THI is utilized in various research concerning thermal comfort, both to prevent work disturbances and to assess outdoor thermal comfort. Furthermore, THI is also used in research to optimize building designs, such as in religious buildings. Its application can extend to other contexts, such as evaluating thermal comfort inside motor vehicles, in public spaces, in open areas, and in spaces with high occupancy density, such as mosques. Additionally, THI is used in research to predict the effects of climate change on thermal comfort in specific regions.

3.2. Increases The Potential for Carbon Absorption and Its Ability to Reduce UHI

3.2.1. Vegetation Carbon Reserves

Based on the survey results, vegetation measurement data were obtained, as presented in the appendix. Following data processing, results were obtained for Carbon Storage Potential (kg/pixel) for each sample plot as shown in table 4 below.

Table 4. Carbon Storage Potential (kg/pixel) per Sample Plot

No.	Plot Number	NDVI Value	Total Carbon (kg/pix)	No.	Plot Number	NDVI Value	Total Carbon (kg/pix)
1	10	0,27	10,62	18	35	0,46	103,69
2	11	0,26	7,91	19	39	0,46	124,16
3	12	0,32	10,40	20	40	0,48	152,18
4	13	0,36	8,43	21	41	0,45	108,97
5	15	0,36	30,68	22	42	0,53	148,14
6	16	0,36	56,27	23	44	0,54	200,97
7	17	0,35	28,40	24	46	0,53	160,68
8	18	0,37	43,92	25	48	0,50	254,15
9	19	0,36	60,45	26	49	0,54	133,59
10	20	0,39	23,73	27	51	0,56	357,09
11	22	0,35	29,70	28	56	0,65	419,41
12	24	0,39	60,08	29	57	0,61	398,18
13	25	0,35	39,08	30	59	0,64	450,71
14	28	0,45	27,48	31	60	0,61	412,44
15	31	0,45	87,71	32	62	0,65	452,22
16	32	0,47	138,44	33	63	0,63	298,13
17	34	0,43	99,59	34	64	0,63	295,59
				35	68	0,73	646,20

Based on table 4, the data shows a correlation between NDVI and carbon storage potential in vegetation, measured in kilograms per pixel (assuming a pixel size of 10m x 10m). NDVI is a commonly used indicator to assess the density and health of vegetation, with higher NDVI values indicating denser and healthier vegetation. NDVI is an important indicator for monitoring vegetation dynamics due to its relationship with above-ground biomass, thus underpinning the relationship between NDVI and carbon storage. From the data presented, it is observed that NDVI values range from 0.26 to 0.73, indicating variations in vegetation density at different locations. Plots with higher NDVI values generally have greater total carbon, indicating that areas with denser vegetation tend to have higher carbon storage potential. For example, Plot Number 68 with an NDVI of 0.73 has the highest total carbon in the table at 646.20 kg per pixel, while Plot Number 11 with an NDVI of 0.26 has one of the lowest total carbons at 7.91 kg per pixel. The results listed are statistically processed into a Model of NDVI Value Relationship with Total Carbon (kgC/100m²) which shown in figure 7 below.

 ISSN 2723-6471

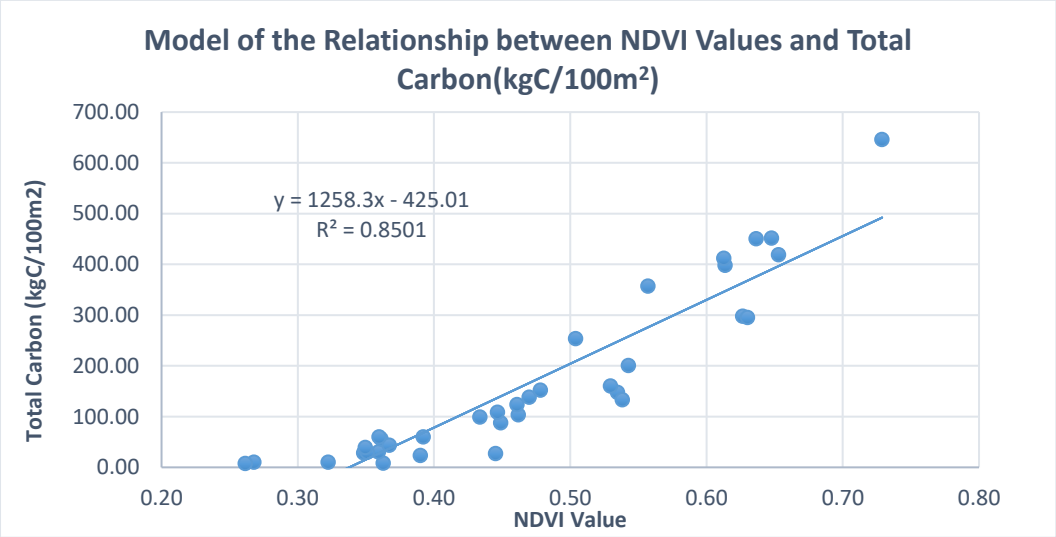

Figure 7. Model of NDVI Value Relationship with Total Carbon

The graph in figure 7 shows the model of the relationship between the NDVI and Total Carbon measured in kilograms per 100 square meters. The plotted data show a positive correlation between NDVI and carbon content in vegetation, reflected in an upward trend: as NDVI increases, the total stored carbon also tends to increase. This emerging pattern indicates a positive relationship between NDVI and carbon storage: as NDVI increases, the total stored carbon also tends to increase. This is consistent with the understanding that denser vegetation, indicated by higher NDVI, typically has a greater capacity to absorb and store carbon from the atmosphere through photosynthesis. In this model, the listed linear regression equation is y = 1258.3x - 425.01. This equation indicates that for each one-point increase in NDVI value, the total stored carbon increases by approximately 1258.3 kg per 100m², after being offset by a constant factor of -425 kg per 100m². This suggests that vegetation with higher NDVI has the potential to store more carbon. The determination coefficient (R^2) is 0.850, indicating that about 85% of the variation in total stored carbon can be explained by this regression model based on NDVI values. This is a strong indication that NDVI is a good predictor for estimating carbon content in vegetation. Additionally, the mentioned Pearson correlation value is 0.92, indicating a very strong relationship between NDVI and total carbon. A correlation value close to 1 indicates that the relationship between the two variables is very close, with higher NDVI values consistently correlating with increased carbon content. This figure provides a clear visual representation of the positive relationship between vegetation indicated by NDVI and carbon storage potential. This statement is in line with research suggesting that NDVI can reflect changes in vegetation cover and productivity, thereby impacting carbon dynamics. To confirm that the model is acceptable, a validation test of the above model was conducted. In this study, validation has been carried out to test the accuracy of the formula in a model. The validation test results are presented in table 5 below.

Table 5. Model Validation Test Results for the Relationship of NDVI Value with Total Carbon

Numb	Plot Number	NDVI Value	Actual Value	Estimation Value	Difference
1	14	0,37	5,44	37,9	1051,2
2	21	0,34	22,83	2,5	413,8
3	23	0,37	18,76	42,2	549,2
4	26	0,42	26,27	98,6	5236,2
5	27	0,45	13,63	144,9	17231,3
6	29	0,46	22,38	154,3	17395,6
7	30	0,43	26,67	112,3	7328,3
8	33	0,43	43,84	119,8	5774,5
9	36	0,44	532,05	128,0	163236,3

 ISSN 2723-6471

10	37	0,47	55,45	170,0	13126,3
11	38	0,47	50,82	168,7	13903,5
12	43	0,55	66,45	270,4	41587,5
13	45	0,57	47,50	298,1	62774,7
14	47	0,54	53,66	260,1	42620,3
15	50	0,58	416,36	298,5	13887,3
16	52	0,54	123,28	256,1	17639,2
17	53	0,54	112,81	250,4	18939,3
18	54	0,53	119,44	245,7	15932,7
19	55	0,65	188,60	388,6	39982,1
20	58	0,65	2282,14	399,0	3546303,5
21	61	0,62	572,35	354,0	47658,4
22	65	0,65	202,13	395,0	37191,2
23	66	0,64	1094,72	382,8	506846,3
24	67	0,72	228,27	476,1	61417,1
				Average	195751,1
				RMSE	442,4

The actual value represents the carbon amounts calculated from vegetation survey data collected in the field. The estimated value is derived from the application of a formula (model equation). From these two sets of data, the average difference was calculated, and RMSE and Normalized Root Mean Squared Error (NRMSE) were determined to be 0.23%. The validation results of the model are considered accurate because the NRMSE value is less than 1%. Subsequently, the data were processed spatially to estimate the overall carbon potential in the city of Banjarbaru, which is displayed in figure 8 below.

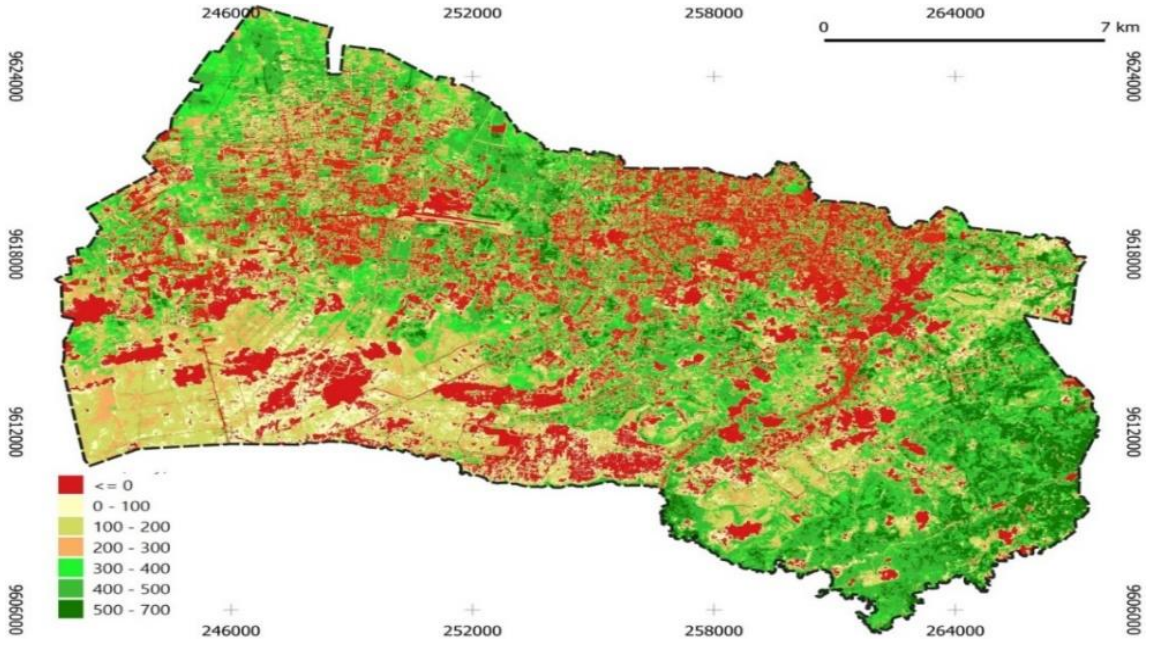

Figure 8. Carbon Storage Potential Classes (Kg C/pixel)

Figure 8 is a map that shows the distribution of carbon storage potential in the research area, measured in kilograms per pixel. The map uses a color scheme to depict various levels of carbon storage potential, with the values provided

 ISSN 2723-6471

in the map legend. Green colors on the map indicate areas with lower carbon storage potential, ranging from 0 to 100 kg per pixel. The darker the green, the higher the storage potential, reaching up to 200 kg per pixel. Light pink to dark red indicates increasingly higher carbon storage potential, with the particularly dark red areas showing very high carbon storage potential, ranging from 500 to 700 kg per pixel.

In the context of the distribution of vegetation carbon storage potential in urban areas relative to changes in vegetation cover and surface temperature levels. Green infrastructure is considered to have the potential to reduce the effects of UHI and other climate change impacts. The decline in environmental quality in urban areas is caused by the reduction of space for vegetation due to rapid urbanization. Other studies indicate that changes in land cover can affect surface temperatures in urban areas, with urban areas tending to have higher temperatures than more vegetated rural areas. These changes are influenced by factors such as the loss of vegetation cover and the expansion of residential land. The relationship between vegetation density and building with surface temperatures in urban areas. The decreasing proportion of vegetation due to land use change can contribute to the UHI phenomenon. Thus, these studies provide deeper insights into how the distribution of urban vegetation carbon storage potential can be influenced by changes in vegetation cover and surface temperature levels.

3.2.2. Vegetation Carbon Emissions / Uptake From 2020-2023

Reviewing the carbon absorption conditions in the city of Banjarbaru, one can observe the carbon absorption over the last four years, from 2020 to 2023, as presented in figure 9 below.

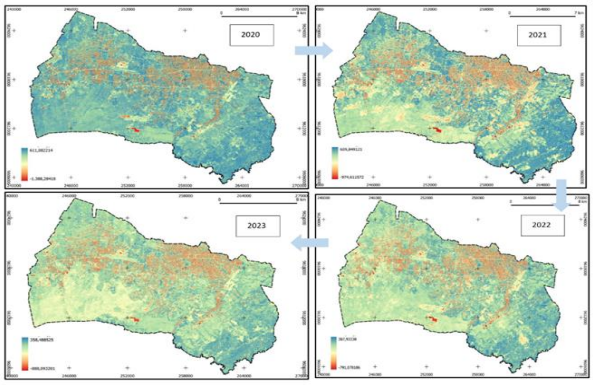

Figure 9. Vegetation Carbon Emission/Absorption from 2020 to 2023

The map in figure 9 contains information on Banjarbaru's carbon reserves from 2020, 2021, 2022, and 2023. On the map, green colors indicate areas with larger vegetation carbon reserves; the darker the green, the greater the carbon stored in that area. Conversely, red colors represent areas with lower carbon reserves, with darker red indicating fewer carbon reserves in those areas. The magnitude of the stored peat potential can be seen from the legend for each year. In 2020, carbon absorption reached the highest value of approximately 611 kgC/100m². However, carbon absorption values continued to decline in the following years, with a drastic decrease in 2022, falling to 307 kgC/100m² from 609 kgC/100m² in 2021. In 2020, carbon absorption reached its peak, but significant decreases were observed in subsequent years. This decline could be due to climate change and land-use changes that commonly occur in urban areas. Additionally, population growth and rapid urban expansion also contribute to land-use changes and reduced carbon absorption. Studies have also shown that landscape changes due to urbanization can affect carbon sequestration rates, where urban trees generally have higher carbon sequestration rates than other green spaces due to a higher leaf area index. Grass cutting and natural conditions such as lack of rainfall also impact. Although urban green spaces can function as carbon sinks through photosynthesis, there is a negative tendency towards shrubbery among local communities due to low productivity and susceptibility to fire. Furthermore, land-use changes from forest to agriculture and urban areas can also lead to a decrease in carbon reserves.

Therefore, to address the decline in carbon storage potential in urban areas, greater efforts are needed to change the current conditions both socially and physically, such as increasing green spaces, managing land use wisely, and paying attention to population growth and sustainable urban expansion. Furthermore, additional research is needed to understand the impact of urbanization on carbon reserves and to develop effective strategies to balance urban growth

 ISSN 2723-6471

with environmental conservation. The decreasing carbon reserves observed over the years are expected to continue diminishing as time progresses. Land changes, deforestation, forest degradation, and other human activities are some of the causes of the significant reduction in carbon reserves.

3.3. Wireless Sensor Networks Analysis Data

Based on the results of the analysis from increases the Potential for Carbon Absorption and Its Ability to Reduce UHI. Field data were collected using a WSN based on NDVI classes, which were analyzed using satellite imagery. This dataset provides real-time representations of field conditions from areas corresponding to the data obtained via Sentinel-2 imagery. Sensor data encompass air temperature and humidity, soil temperature and humidity, and concentrations of CO and CO2. This dataset is analyzed to calculate carbon emissions and absorption potentials in real-time. The analysis of field data serves to validate satellite-derived data, leading to the development of a model that is validated against real-time field data through a WSN. Results indicate that carbon emissions and absorption can be effectively analyzed using data captured by sensors installed at coordinate points previously classified via satellite imagery. Figure 10 below shown progress while analyzing realtime data using WSN.

Rata-Rata Nilai CO2	502.826304 ppm
Rata-rata Serapan (grC)	-0.0093988575
tonC/14m²/hari	-0.0000000010
tonC/ha/hari	-0.0000006849
tonC/ha/tahun	-0.0002499781

ID	Waktu	Nilai CO2 (ppm)	Perubahan CO2 (ppm)	Mol CO2	Massa C (grC/ruang)	Emisi (grC)	Serapan (grC)
1051071	2024-02-12 10:59:00	569	0.000000	0.000000	0.000000	0.000000	0.000000
1051072	2024-02-12 10:59:01	569	-1.000000	-0.000630	-0.007562	0.000000	-0.007562
1051073	2024-02-12 10:59:02	568	0.000000	0.000000	0.000000	0.000000	0.000000
1051074	2024-02-12 10:59:02	568	0.000000	0.000000	0.000000	0.000000	0.000000
1051075	2024-02-12 10:59:03	568	-1.000000	-0.000630	-0.007562	0.000000	-0.007562
1051076	2024-02-12 10:59:04	567	0.000000	0.000000	0.000000	0.000000	0.000000
1051077	2024-02-12 10:59:04	567	0.000000	0.000000	0.000000	0.000000	0.000000
1051078	2024-02-12 10:59:05	567	-1.000000	-0.000630	-0.007562	0.000000	-0.007562
1051079	2024-02-12 10:59:06	566	-1.000000	-0.000630	-0.007562	0.000000	-0.007562

Figure 10. Analysis Realtime Data using WSN

The result presents atmospheric CO2 concentration measurements CO2 concentrations decreased from 569 ppm to 566 ppm, with significant reductions recorded intermittently, reflecting a decrease of 1 ppm at several intervals. The columns labeled 'Mol CO2' and 'Massa C (gr/Cruang)' provide information on the amount of CO2 molecules and the associated carbon mass resulting from these changes. The 'Emisi (grC)' and 'Serapan (grC)' columns indicate that no carbon emissions were detected, and carbon absorption occurred, noted as -0.007562 grams on several measurements. Additionally, the top of the table includes calculations for average and total carbon absorption per day, per hectare per day, and per year, illustrating the rate of carbon sequestration in the observed area during the measurement periode.

3.4. Low Carbon Green City Design Based on Land Cover

Based on the results of the analysis from Objective 1, which emphasizes high UHI effects and high THI levels supported by Objective 2, which presents a low potential for carbon sequestration (as per the research findings) Objective 3 aims to address both Objective 1 and Objective 2. This is achieved by improving thermal discomfort and enhancing carbon sequestration through designs that focus on increasing biomass with a foundation in spatial and economic concepts:

1) Urban farming
2) Green building
3) Green corridors

The impact of these three concepts contributes to the enhancement of carbon stocks and further reduction of greenhouse gases, leading to potential engagement in carbon trading.

4. Conclusion

This research presents a design for a low-carbon green city based on vegetation in Banjarbaru using Sentinel-2 imagery, encompassing various aspects. The study successfully demonstrates that increasing vegetation cover significantly aids

in mitigating the UHI effect and enhancing carbon sequestration in urban environments. Detailed analyses employing GIS, field data, and real-time data via WSN emphasize the critical role of urban greenery in reducing local air temperatures and enhancing urban livability. Furthermore, the study highlights the potential of green infrastructure to function as carbon sinks, absorbing CO2 emissions and contributing to climate change mitigation. Through methodological advancements and practical applications, this research makes a significant contribution to urban planning and environmental management strategies aimed at fostering sustainable urban environments.
In the context of Banjarbaru, a green city refers to an urban area designed to optimize green spaces, reduce carbon emissions, and enhance residents' quality of life through strategic vegetation planting and the use of green technologies. This includes the implementation of international standards such as ICLEI's Green Climate Cities program and the World Business Council for Sustainable Development's Urban Infrastructure Initiative. Technological advancements, such as the use of drones for vegetation mapping and the development of more advanced sensors for monitoring temperature and humidity, can enhance the effectiveness of future UHI mitigation and carbon sequestration strategies. The results of this study strongly suggest that the strategic placement of vegetation in urban planning can greatly improve thermal comfort and enhance carbon sequestration. We've pinpointed specific areas within Banjarbaru where adding more greenery could significantly cool down densely built-up areas currently suffering from high temperatures due to a lack of green cover. This research provides a validated model for other cities similar to Banjarbaru to follow, emphasizing the necessity of integrating environmental considerations into urban development to address the challenges posed by climate change and urbanization. This model can serve as a benchmark for developing future urban planning policies that prioritize green infrastructure, thereby enhancing both the ecological and social fabric of urban areas.

5. Declarations

5.1. Author Contributions

Conceptualization: H.D.N., A.R.S., G.M.H., and A.N.; Methodology: H.D.N.; Software: A.R.S.; Validation: H.D.N., A.R.S., G.M.H., and A.N.; Formal Analysis: H.D.N., A.R.S., G.M.H., and A.N.; Investigation: H.D.N.; Resources: A.R.S.; Data Curation: G.M.H.; Writing Original Draft Preparation: H.D.N. and A.N.; Writing Review and Editing: H.D.N. and A.N.; Visualization: A.N.; All authors have read and agreed to the published version of the manuscript.

5.2. Data Availability Statement

The data presented in this study are available on request from the corresponding author.

5.3. Funding

The authors received no financial support for the research, authorship, and/or publication of this article.

5.4. Institutional Review Board Statement

Not applicable.

5.5. Informed Consent Statement

Not applicable.

5.6. Declaration of Competing Interest

The authors declare that they have no known competing financial interests or personal relationships that could have appeared to influence the work reported in this paper.

References

[1] S. Jevrejeva, L. Jackson, R. Riva, A. Grinsted, and J. C. Moore, "Coastal Sea Level Rise With Warming Above 2 °C," *Proc. Natl. Acad. Sci.*, vol. 113, no. 47, pp. 13342–13347, 2016, doi: 10.1073/pnas.1605312113.

[2] G. A. Meehl *et al.*, "How Much More Global Warming and Sea Level Rise?," *Science (80-.).*, vol. 307, no. 5716, pp. 1769–1772, 2005, doi: 10.1126/science.1106663.

[3] S. Kandel, B. Gyawali, J. Sandifer, S. Shrestha, and S. Upadhaya, "Assessment of Urban Heat Islands (UHIs) Using Satellite-

Derived Normalized Difference Vegetation Index (NDVI), and Land Surface Temperature (LST) in Three Metropolitan Cities of Nepal," *Banko Janakari*, vol. 32, no. 2, pp. 37–51, 2022, doi: 10.3126/banko.v32i2.50895.

[4] S. Taslim, D. M. Parapari, and A. Shafaghat, "Jurnal Teknologi Full paper Urban Design Guidelines to Mitigate Urban Heat Island (UHI) Effects In Hot-," *J. Teknol.*, vol. 4, no. 7, pp. 119–124, 2015.

[5] M. Pena Acosta, M. Dikkers, F. Vahdatikhaki, J. Santos, and A. G. Dorée, "A comprehensive generalizability assessment of data-driven Urban Heat Island (UHI) models," *Sustain. Cities Soc.*, vol. 96, no. 1, p. 104701, 2023.

[6] D. Sun and M. Kafatos, "Note on the NDVI-LST relationship and the use of temperature-related drought indices over North America," *Geophys. Res. Lett.*, vol. 34, no. 24, 2007, doi: https://doi.org/10.1029/2007GL031485.

[7] Y. Lu, M. A. Rahman, N. W. Moore, and A. J. Golrokh, "Lab-Controlled Experimental Evaluation of Heat-Reflective Coatings by Increasing Surface Albedo for Cool Pavements in Urban Areas," *Coatings*, 2021.

[8] H. K. Jabbar, M. N. Hamoodi, and A. N. Al-Hameedawi, "Urban heat islands: a review of contributing factors, effects and data," *IOP Conf. Ser. Earth Environ. Sci.*, vol. 1129, no. 1, p. 12038, 2023, doi: 10.1088/1755-1315/1129/1/012038.

[9] Munsyi, A. Sudarsono, and M. U. H. Al Rasyid, "Secure Data Exchange Based on Wireless Sensor Network for Environmental Monitoring Using Dynamical Attributed Based Encryption," *Int. J. Adv. Sci. Eng. Inf. Technol.*, vol. 11, no. 4, pp. 1306–1315, 2021, doi: 10.18517/ijaseit.11.4.8546.

[10] BHARTENDU SAJAN, SHRUTI KANGA, SURAJ KUMAR SINGH, VARUN NARAYAN MISHRA, and BOJAN DURIN, "Spatial variations of LST and NDVI in Muzaffarpur district, Bihar using Google earth engine (GEE) during 1990-2020," *J. Agrometeorol.*, vol. 25, no. 2 SE-Research Paper, pp. 262–267, May 2023, doi: 10.54386/jam.v25i2.2155.

[11] Z. KHAN and A. JAVED, "Correlation between land surface temperature (LST) and normalized difference vegetation index (NDVI) in Wardha Valley Coalfield, Maharashtra, Central India," *Nov. Geod.*, vol. 2, no. 3 SE-Research articles, p. 53, Sep. 2022, doi: 10.55779/ng2353.

[12] K. Gadekar, C. B. Pande, J. Rajesh, S. D. Gorantiwar, and A. A. Atre, "Estimation of Land Surface Temperature and Urban Heat Island by Using Google Earth Engine and Remote Sensing Data BT - Climate Change Impacts on Natural Resources, Ecosystems and Agricultural Systems," C. B. Pande, K. N. Moharir, S. K. Singh, Q. B. Pham, and A. Elbeltagi, Eds. Cham: Springer International Publishing, 2023, pp. 367–389. doi: 10.1007/978-3-031-19059-9_14.

[13] N. da Silva Espinoza *et al.*, "Assessment of urban heat islands and thermal discomfort in the Amazonia biome in Brazil: A case study of Manaus city," *Build. Environ.*, vol. 227, no. August 2022, p. 109772, 2022.

[14] A. D. Sakti *et al.*, "Spatial Prioritization for Wildfire Mitigation by Integrating Heterogeneous Spatial Data: A New Multi-Dimensional Approach for Tropical Rainforests," *Remote Sens.*, vol. 14, no. 3, 2022, doi: 10.3390/rs14030543.

[15] K. Onačillová, M. Gallay, D. Paluba, A. Péliová, O. Tokarčík, and D. Laubertová, "Combining Landsat 8 and Sentinel-2 Data in Google Earth Engine to Derive Higher Resolution Land Surface Temperature Maps in Urban Environment," *Remote Sens.*, vol. 14, no. 16, pp. 1-12, 2022, doi: 10.3390/rs14164076.

[16] R. Rahmadanti, A. Jauhari, D. M. Asy'ari Program, and S. Kehutanan, "Distribution of Urban Heat Island at Banjarbaru Using Remote Sensing," *J. Sylva Sci.*, vol. 05, no. 2, pp. 194–202, 2022.

[17] S. Guha, H. Govil, and P. Diwan, "Monitoring LST-NDVI Relationship Using Premonsoon Landsat Datasets," *Adv. Meteorol.*, 2020, doi: 10.1155/2020/4539684.

[18] Y. Deng *et al.*, "Relationship Among Land Surface Temperature and LUCC, NDVI in Typical Karst Area," *Sci. Rep.*, vol. 1, no. 1, pp. 1-9, 2018, doi: 10.1038/s41598-017-19088-x.

[19] B. Halder, J. Bandyopadhyay, and P. Banik, "Evaluation of the Climate Change Impact on Urban Heat Island Based on Land Surface Temperature and Geospatial Indicators," *Int. J. Environ. Res.*, vol. 15, no. 5, pp. 819–835, 2021.

[20] K. Masumoto, "Urban Heat Islands BT - Environmental Indicators," *R. H. Armon and O. Hänninen, Eds. Dordrecht: Springer Netherlands*, 2015, pp. 67–75. doi: 10.1007/978-94-017-9499-2_5.

[21] W. B. Adi, Sukuryadi, J. S. Adiansyah, Ibrahim, and H. I. Johari, "Analisis Pola Spasial Fenomena Urban Heat Island (Uhi) Berdasarkan Faktor Emisivitas Lahan," *Geography*, vol. 10, no. 2, pp. 6–7, 2022, [Online]. Available: http://journal.ummat.ac.id/index.php/geography/article/view/9740